JOURNAL OF MATERIALS SCIENCE 25 (1990) 2144–2148

Effects of residual stresses on the failure micromechanisms in toughened epoxy systems

I. M. LOW
Department of Chemical and Materials Engineering, University of Auckland, Private Bag, Auckland, New Zealand

The residual stress–strain distributions in various toughened epoxy systems have been analysed and related to their failure micromechanisms. The thermal expansion mismatch between epoxy and dispersed fillers gives rise to either compressive or tensile radial stresses at the interface. The interplay of these and the crack–tip stresses can profoundly govern the nature of crack tip–filler interactions which in turn dictate the micromechanisms of failure. Control of these stresses may be tailored to improve the fracture resistance and crack growth stability of toughened epoxies.

1. Introduction

Epoxy resin like glasses are brittle materials with very poor fracture resistance ($K_{\mathrm{IC}} \leqslant 1\,\mathrm{MPa\,m^{1/2}}$). In an attempt to improve the fracture resistance of epoxy resins, various types of dispersion phases have been deliberately introduced which include; (a) rigid particulates [1–3], (b) rubbery particles [4–6] and (c) hybrid rigid and rubbery particles [7, 8]. Considerable enhancement of fracture toughness has been recorded in these modified epoxies particularly for the dispersion system (c) where K_{IC} values of up to $3.0\,\mathrm{MPa\,m^{1/2}}$ were achieved [8].

Various toughening mechanisms have been advanced to account for the improvement of fracture resistance in these toughened epoxy systems. Absorption of energy from crack deflection [9], crack pining [10] and brittle fracture of particulates [11] have been attributed to improved toughness attained by epoxies containing dispersion system (a). Toughening mechanisms in epoxies with dispersion systems (b) and (c) are more complex. The former includes: stretching, debonding and tearing of rubber particles [6], crazing [12] and yielding near the crack tip [4, 5, 13]. The latter is believed to encompass the combined and perhaps synergistic failure processes encountered in dispersion systems (a) and (b) [7].

All the toughening mechanisms proposed above have neglected the significance of thermal expansion characteristics of the dispersed phases in particular the thermal expansion coefficient (α) which may result in generation of large residual stresses at the interface between the epoxy matrix and the dispersed phase. The presence of these stresses at the interface due to thermal expansion mismatch will to a large extent, determine the non-planarity of the crack path. A tortuous crack path will absorb more energy in the surface production and the fracture toughness will be improved and vice versa. This concept has been well utilized to control the fracture toughness of glass-ceramics which contain fine crystals uniformly dispersed in or bonded by the residual glass [14]. The degree and nature of these stresses developed at the interface between crystal and glass due to thermal expansion mismatch will dictate a crack to propagate either by transgranular or intergranular fracture. Clearly, the phenomenon of thermal expansion mismatch is of vital importance in the control of fracture toughness of multiphase brittle materials such as glass ceramics and particulate-modified epoxies. In the latter, the dispersed phases have values of thermal expansion coefficient (α) vastly different from that of the epoxy matrix ($\alpha_{\mathrm{E}} = 65 \times 10^{-6}\,{}^{\circ}\mathrm{C}^{-1}$). The rigid particulates have α_{p} values less than $10 \times 10^{6}\,{}^{\circ}\mathrm{C}^{-1}$ while rubbery particles have α_{R} value of around $90 \times 10^{-6}\,{}^{\circ}\mathrm{C}^{-1}$ [15]. In view of the large thermal expansion mismatch in most toughened epoxy systems, it is the intention of this paper to highlight an alternative or additional toughening mechanism in these epoxies by virtue of mismatch in the thermal expansion characteristics. This phenomenon is subsequently employed to model the failure processes observed.

2. Experimental procedure

The epoxy resin employed was GY250, a diglycidyl ether of bisphenol A (DGEBA) supplied by Ciba Geigy. The curing agent was piperidine and the rubber employed was a carboxyl-terminated, random copolymer of butadiene and acrylonitrile, CTBN (1300 × 13), obtained from BF Goodrich. The rigid fillers were commercial short alumina fibres (≈ 5 mm long and $5\,\mu$m in diameter) and fine metastable zirconia powders. The latter was derived from calcination of commercial purity zirconyl chloride at the appropriate temperature. The formulations of the various epoxy systems studied are depicted in Table I.

Details of the preparation and testing of epoxy samples were reported elsewhere [16]. Essentially, sheets of the epoxy sample (6 mm thick) were prepared by casting in a greased metal mould which was then heated for 16 h at 120° C. Compact-tension specimens from these sheets were tested in an Instron machine at

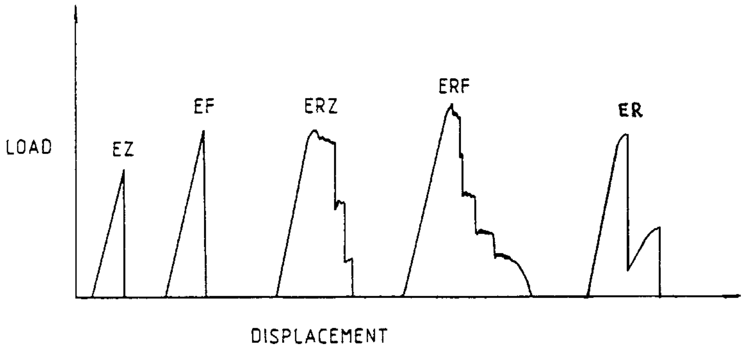

Figure 1 Load plotted against displacement for various toughened epoxies.

a displacement rate of 1.0 mm min^{-1} to ascertain the fracture toughness and the crack growth behaviour. The resultant fracture surfaces were coated with platinum for examination under a Joel 35-C scanning electron microscope.

3. Results

Epoxy–zirconia (EZ) and epoxy–fibre (EF) specimens displayed catastrophic brittle fracture with no apparent stress-whitening on the fractured surface (Fig. 1). On the other hand, epoxy–rubber (ER), epoxy–rubber–zirconia (ERZ) and epoxy–rubber–fibre (ERF) materials displayed some non-linearity in the load–displacement curve (Fig. 1) prior to the fracture instability. The phenomenon of crack jumping or "stick–slip" appeared to operate in these epoxies containing dispersed rubbery particles which became more pronounced in the presence of a third rigid filler, especially the short fibres. The fractured surface of ER specimen displayed a stress-whitened zone SWZ ($\leqslant 2$ mm) which became more extensive in the ERZ specimen ($\simeq 4$ mm). Stress whitening was most extensive in the ERF specimen where the SWZ covered almost the whole fracture surface. There appears to be a direct relationship between the extent of stress-whitening and the degree of non-linearity observed in the load–displacement curve.

Table II shows the values of fracture toughness (K_{IC}) displayed by the various modified epoxy materials. Only a very slight improvement in fracture toughness was recorded for epoxy containing metastable ZrO_2 particles. A much higher value was obtained when short Al_2O_3 fibres were used. Addition of 15 phr rubber raised the K_{IC} value of epoxy from 0.8 to 2.1 MPa m$^{1/2}$. Hybrid dispersion of rubber and ZrO_2 improved the fracture resistance further. The best improvement was recorded for ERF materials with K_{IC} value of about 4.0 MPa m$^{1/2}$.

The fracture surfaces of both EZ and EF materials displayed the characteristics of crack–tip pinning by the rigid ZrO_2 particles and short Al_2O_3 fibres respectively (Fig. 2). The microcracking of epoxy matrix tangential to the fibre is clearly depicted in Fig. 3a. The ease of shear stresses induced by polishing in causing premature debonding and complete removal of ZrO_2 particles from the epoxy matrix is illustrated by Fig. 3b. In the presence of rubbery particles, both ZrO_2 particles and short Al_2O_3 fibres appeared less effective in causing crack–tip pinning (Fig. 4). Fibre pull-outs and interface debonding were clearly displayed on the fracture surface of ERF specimen in contrast to the EF specimen.

4. Discussion

4.1. Theoretical aspects

The differential thermal expansion is a very important parameter in any multiphase or composite system since it determines the residual stress–strain distributions after fabrication and can have overriding effects on the resultant mechanical and fracture properties [14]. Large stresses can be developed at the interface between the matrix and the dispersed phase due to thermal expansion mismatch. The magnitude of these stresses, both radial (σ_r) and tangential (σ_t), may be estimated from [17]

$$-\sigma_r = 2\sigma_t = \frac{\Delta\alpha\,\Delta T}{(1 + \nu_m/2E_m) + (1 - 2\nu_f/E_f)} \qquad (1a)$$

$$\simeq \Delta\alpha\Delta T E_m \qquad (1b)$$

where α, T, ν and E are the linear thermal expansion coefficient, temperature, Poisson's ratio and elastic modulus respectively. The subscripts refer to the matrix (m) and dispersed filler (f).

The nature of these stresses depends strictly on the thermal expansion characteristics of the phases at the interface. When $\alpha_f < \alpha_m$, the stresses at the interface are compressive in the radial directions in both phases but in the circumferential directions they are tensile in the matrix and compressive in the filler. The compressive stress in the interface would cause a crack approaching from the matrix to propagate across the

TABLE I Formulations of various epoxy systems

Material	Composition (phr)*
Epoxy	100
Piperidine	5
CTBN rubber	0 or 15
Zirconia powder	0 or 25
Al_2O_3 fibres	0 or 19

*phr = parts per hundred of resin by weight.

TABLE II Fracture toughness of various epoxy systems

Material	K_{IC} (MPa m$^{1/2}$)
E	0.8
EZ	0.96
EF	2.55
EF	2.10
ERZ	2.84
ERF	3.85

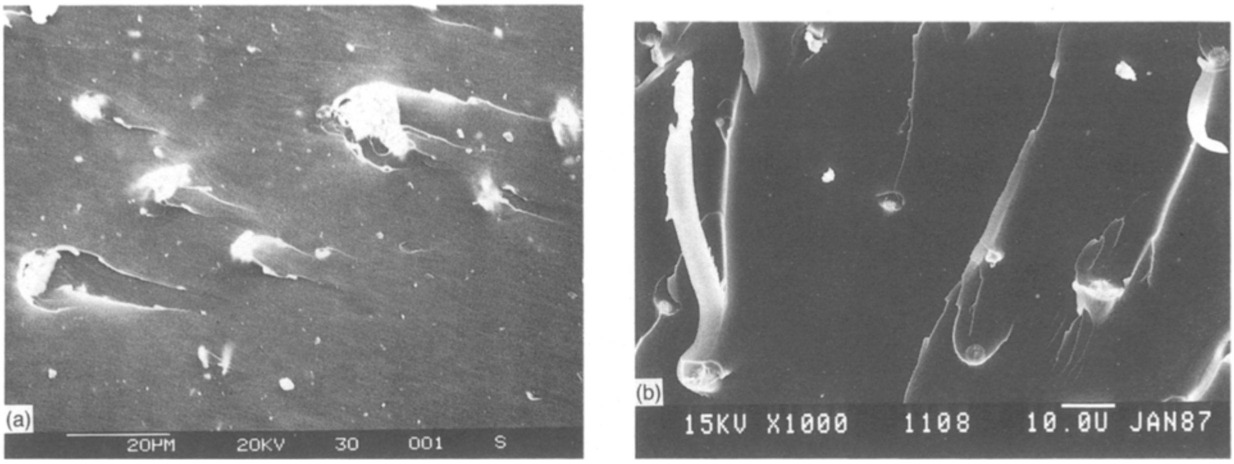

Figure 2 Fracture surfaces of (a) epoxy–ZrO_2 (EZ) system showing crack pinning and (b) epoxy–fibre (EF) system showing crack pinning and fibre fracture.

strongly bonded interface to cause transgranular fracture. This more direct path results in a lower fracture toughness. On the other hand, when $\alpha_f > \alpha_m$ the interface will be subject to radial tensile stresses. Two effects are possible depending on the strength of the filler–matrix interface. If the interface is strong enough, the fillers will endeavour to strain the matrix in compression in the axial direction; this will increase the overall strain required to initiate failure and hence will result in an improvement in the fracture strength and toughness. Conversely, if the interface strength is not strong, interfacial debonding will occur and fracture will invariably be intergranular. Again, a higher fracture toughness may be obtained due to a longer and more tortuous crack path.

The concept of utilizing thermal expansion mismatch to generate compressive stresses in the matrix has been widely used to strengthen silica glasses by flame polishing [18]. Similar beneficial compressive stresses may be obtained by tempering or ion-exchange of glasses [18] and phase transformation of crystals as in partially stabilized zirconias (PSZ) [19]. This concept is employed in the following discussion as an alternative origin of failure processes in the various epoxy systems studied.

4.2. Epoxy systems containing rigid fillers

In the epoxy systems modified with fillers of ZrO_2 (EZ) and Al_2O_3 (EF), $\Delta\alpha$ is negative ($\alpha_{ZrO_2} = 9.5 \times 10^{-6}\,°C^{-1}$; $\alpha_{Al_2O_3} = 8.5 \times 10^{-6}\,°C^{-1}$). It follows from Equation 1b that compressive radial stresses of about 16.7 and 17.0 MPa respectively are induced at the filler–matrix interface on cooling from the curing temperature of 120° C. These stresses serve to enhance the intrinsic bond developed at the interface. Consequently, processes for premature debonding at the interface in the vicinity of an advancing crack tip are suppressed. The stress fields surround the ZrO_2 particles or Al_2O_3 fibres serve to cause the crack front to be pinned and bowed before breaking away to produce "tail ends" which are the characteristic features of crack pinning (Fig. 2). The strong bonding at the interface also provides an efficient stress transfer from the matrix to the filler. In the EF system, the large aspect ratio of Al_2O_3 fibres ($\simeq 1000$) allows a rapid building up of tensile stresses which will fracture the fibres when the ultimate tensile strength of the fibre is exceeded. Fibre debonding and pull-out are thus unlikely. The near spherical ZrO_2 particles in the EZ system will almost prevent the building up of stresses to exceed their fracture strength. The crack front will invariably either deflect or shear through the interface. This absence of premature interface debonding is believed to prevent the formation of stress-whitening during cracking, resulting in an unstable and catastrophic fracture with planar fracture surface. The

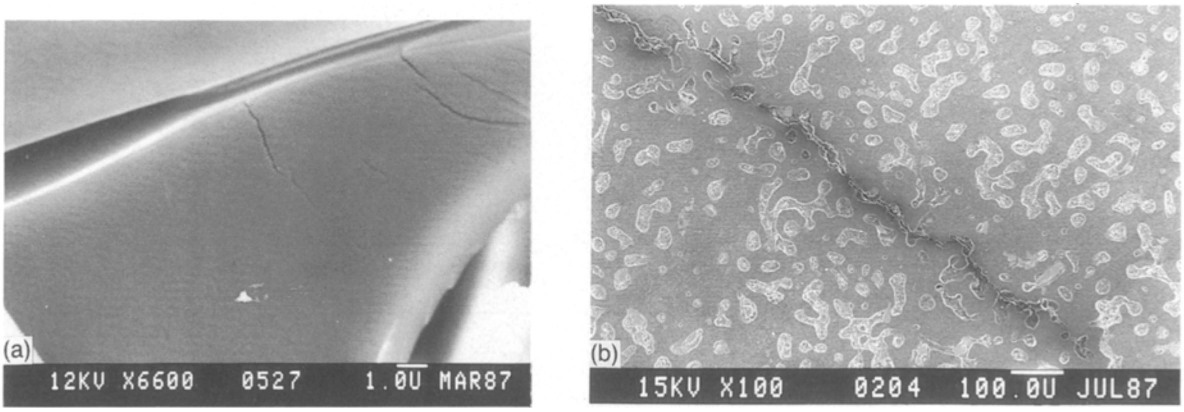

Figure 3 (a) Formation of microcracks in the epoxy matrix containing short Al_2O_3 fibres. (b) Particle debonding in a polished surface of epoxy matrix containing metastable ZrO_2 particles.

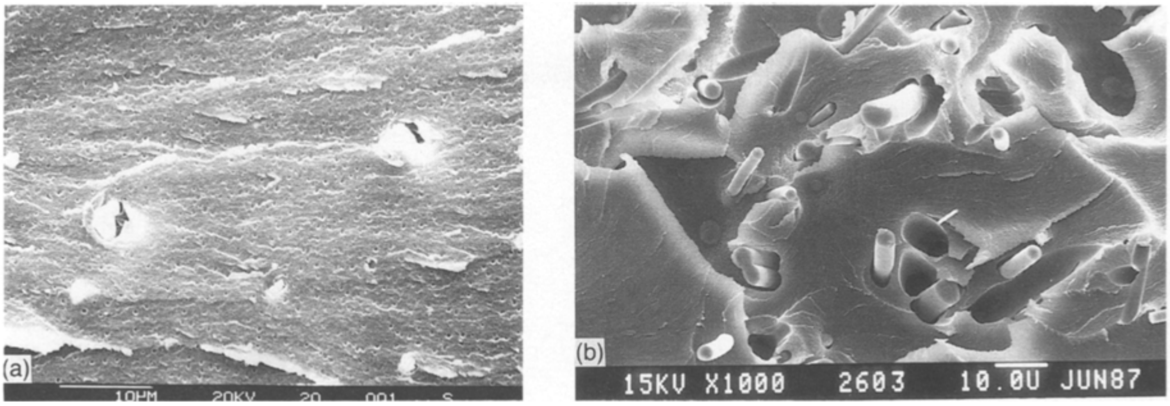

Figure 4 Fracture surfaces of (a) epoxy–rubber–ZrO_2 (ERZ) showing a much reduced crack-pinning effect and (b) epoxy–rubber–fibre (ERF) system showing fibre debonding and pull-out.

poor fracture toughness recorded by the EZ system suggests that the principal toughening mechanism arises from work dissipation associated with crack pinning by the ZrO_2 particles. Invariably, phase transformation of these metastable particles had not taken place. The low yield strength of epoxy (σ_y = 100 MPa), the near spherical ZrO_2 particles and the large elastic modulus mismatch serve in concert to prevent the necessary stress transfer by shear to build up stresses larger than the critical transformation stress of these metastable ZrO_2 particles [20]. The large elastic modulus mismatch (ΔE = 197 GPa) would invariably be detrimental in achieving a sufficient shear strength at the interface (Fig. 3). In tandem with the compressive radial stresses at the interface are the presence of tensile tangential stresses in the matrix which are conducive for flaw generation. The formation of microcracking in the matrix of the EF system (Fig. 3a) results from the endeavour of the fibres in keeping the matrix in tension in the axial direction.

4.3. Epoxy systems containing hybrid dispersions

The residual stress–strain distributions become more complicated when both rubbery and rigid fillers are dispersed in the epoxy matrix. This complication arises because the rubbery phase has a larger thermal expansion coefficient than that of epoxy. The converse is true for the rigid phase.

In the rubber-modified epoxy system (ER), $\Delta\alpha$ is negative. Hence, from equation (1b), tensile radial stresses of about 6 MPa are induced at the rubber–matrix interface. The chemical bonding between rubbery particles and matrix ensures a strong interface adhesion which can support the resulting tensile stresses. Consequently, these rubbery particles will endeavour to strain the matrix in compression in the axial direction. Invariably, this will result in an overall strain increase required to initiate failure. The generation of these compressive stresses in the epoxy matrix by rubbery particle may provide an alternative or additional source of work dissipation in rubber-toughened epoxies.

The addition of a third filler with low thermal expansion to the epoxy matrix will complicate the above mechanism. The thermal expansion mismatch effect of the two fillers will be diametrically opposing each other. In the ERF system, tensile stresses of about 6 MPa are induced at the rubber–epoxy interface with the concomitant generation of compressive tangential stress at the surrounding matrix. On the other hand, compressive radial stresses of about 17 MPa are induced at the fibre–matrix interface in concert with the production of tensile tangential stresses in the matrix. However, due to the interference from the rubbery particles, the interface bonding between the fibre and the matrix is somewhat reduced by the presence of tensile radial stresses. Under this circumstance, the tendency for premature debonding at the interface is largely enhanced. This results in a poor stress transfer by shear and only a moderate level of stresses may be built up in the fibres which are insufficient to cause fibre fracture. Hence, those fibres shorter than the critical transfer length (l_c) will be fully pulled out (Fig. 4). The formation of an extensive SWZ in this system is largely due to the concurrent display of debonding at the fibre interface and the cavitation of rubber particles. These newly created free surfaces serve to alter the light refractive index at the SWZ [4]. In this case the crack follows a fibre avoidance path resulting in a highly tortuous fracture surface. Avoidance of fibres by the advancing crack tip is accomplished by the initial tilting at the debonded interface and subsequent twisting of the crack front between fibres [21]. Invariably, these sequential processes of fibre debonding, crack bridging and fibre pull-out will result in the stabilization of crack growth (Fig. 1) and a display of a *R*-curve effect [16].

Similar failure processes are anticipated for the ERZ materials. Again, the presence of tensile radial stresses at the rubber–matrix interface will substantially reduce the bonding strength at the ZrO_2–matrix interface. Consequently, premature debonding at the ZrO_2–matrix interface will be greatly enhanced leading to a substantial loss in the crack pinning capability of these ZrO_2 particles (Fig. 4). The enhanced stress-whitening during cracking in this system arises largely from the combined effects of premature debonding at the ZrO_2–matrix interface and the cavitation of rubbery particles. The energy dissipated during this enhanced stress-whitening is believed to be responsible for the pronounced non-linearity in the load–displacement curve and the enhanced stabilization of crack growth (Fig. 1).

5. Conclusions

The residual stress–strain distributions in the various epoxy systems have been analysed. These residual stresses arise from the thermal expansion mismatch between the epoxy matrix and the dispersed phases. Compressive radial and tensile tangential stresses are generated at the interface when the filler has a lower thermal expansion coefficient (α) than that of epoxy matrix. The reverse is true when the filler has a higher value of α. The former tends to enhance interface bonding and encourage catastrophic unstable cracking, resulting in a planar fracture surface. Conversely, the latter tends to generate desirable compressive stresses in the matrix which will invariably raise the overall strain required to initiate failure. In the presence of hybrid fillers with α higher and lower than that of epoxy, considerable improvement in the fracture resistance and stability may be achieved through an enhanced debonding at the interface and stress whitening.

Acknowledgements

Dr S. Bandyopahayay of MRL (Melb), and Professor Y. W. Mai of Sydney University, both of Australia, kindly provided most of the scanning electron micrographs.

References

1. J. SPANOUDAKIS and R. J. YOUNG, *J. Mater. Sci.* **19** (1984) 473.
2. A. C. MOLONEY, H. H. KAUSCH and H. R. STIEGER, *ibid.* **19** (1984) 1125.
3. L. J. BROUTMAN and S. SAHU, *Mater. Sci. Engng.* **8** (1971) 98.
4. A. J. KINLOCH, S. J. SHAW, D. A. TOD and D. L. HUNSTON, *Polymer* **24** (1983) 1341.
5. A. F. YEE and R. A. PEARSON, *J. Mater. Sci.* **21** (1986) 2462.
6. S. KUNZ-DOUGLASS, P. W. R. BEAUMONT and M. F. ASHBY, *ibid.* **15** (1980) 1109.
7. A. J. KINLOCH, D. L. MAXWELL and R. J. YOUNG, *ibid.* **20** (1985) 4169.
8. D. MAXWELL, R. J. YOUNG and A. J. KINLOCH, *J. Mater. Sci. Lett.* **3** (1984) 9.
9. K. T. FABER and A. G. EVANS, *Acta Metall.* **31** (1983) 565.
10. F. F. LANGE, *Phil. Mag.* **22** (1970) 983.
11. E. E. UNDERWOOD, in "Quantitative Microscopy" edited by R. T. Detoff and F. N. Rhines, (McGraw Hill, New York, 1968) p. 149.
12. J. N. SULTAN and F. J. McGARRY, *Polym. Engng. Sci.* **13** (1973) 29.
13. A. J. KINLOCH and J. G. WILLIAMS, *J. Mater. Sci.* **15** (1980) 987.
14. I. W. DONALD and D. P. W. McMILLAN, *ibid.* **11** (1976) 949.
15. L. H. VAN VLACK, "Elements of Materials Science and Engineering", 4th Edition (Addison-Wesley, Reading, MA, 1980).
16. I. M. LOW, Y. W. MAI, S. BANDYOPADHAYAY and V. M. SILVA, *Materials Forum* **10** (1987) 241.
17. J. SELSING, *J. Amer. Ceram. Soc.* **44** (1961) 419.
18. I. J. McCOLM, "Ceramic Science for Materials Technologists", (Leonard Hill, London, 1983).
19. R. G. GARVIE, R. J. H. HANNICK and C. URBANI, *Ceramurg. Int.* **6** (1980) 19.
20. I. M. LOW, *J. Mater. Sci. Lett.* **7** (1988) 241.
21. K. T. FABER and A. G. EVANS, *Acta Metall.* **31** (1983) 565.

Received 3 January
and accepted 23 August 1989